Geomechanics and Engineering, *Vol. 38, No. 4 (2024) 421-437*
https://doi.org/10.12989/gae.2024.38.4.421

Dynamic stability evaluation of nail stabilised vertical cuts in various site classes

Amrita*, B.R. Jayalekshmi[a] and R. Shivashankar[b]

Department of Civil Engineering, National Institute of Technology Karnataka (NITK), Surathkal, Karnataka - 575025, India

(*Received October 22, 2023, Revised June 3, 2024, Accepted August 13, 2024*)

Abstract. The soil nailing method entails the utilisation of nails to reinforce and stabilise a zone of soil mass. This is widely used for various applications due to its effective performance under various loading conditions. The seismic response of 6m high vertical soil-nailed cut in various site classes under dynamic excitations has been investigated in this study considering various lengths and inclinations of nails. The influence of frequency content of dynamic excitation on the response of structure has been assessed through finite element analysis using time history data of three different earthquakes. The seismic stability of the nailed cut in retaining soil in various sites under El Centro, Kobe and Trinidad earthquake ground motion is evaluated based on maximum acceleration response, maximum horizontal deformation, earth pressure distribution on the wall and maximum axial force mobilised in nails. The optimum nail inclination is identified as 15° and a minimum nail length ratio of 0.7 is essential for a stable vertical cut under dynamic excitations.

Keywords: dynamic excitation; finite element analyses; nail length ratio; soil nailing; vertical cuts

1. Introduction

Excavations have become a common practice in the process of making the natural ground surface suitable for the construction of any structure on it. Soil nailing is an effective solution to retain the vertical cut developed in the ground during excavation and to ensure its stability. This method comprises stabilising vertical cuts by inserting reinforcement bars into the soil mass to be retained. These reinforcement bars are known as soil nails. The mechanism of the method is through tensile force which is mobilised in nails as a consequence of the lateral deformation of soil and shear stress developed between the soil-grout interfaces. The main benefit of this method is that it induces less impact on the environment and other nearby structures. This technique is widely used for various applications due to its effective performance under different loading conditions.

The concept of the soil nailing system started with the stabilization of underground excavation in rock, which was known to be the New Austrian Tunnelling Method (Rabcewicz 1964). The method comprised of inclusion and grouting of passive steel bars or reinforcement into the rock followed by putting on a reinforced shotcrete layer of facing on the surface. This concept of retaining the earth was then used for various rock-slope stabilising projects. The effectiveness and easement of the method made it applicable for the stabilization of slopes and excavations in soil. The characteristics and performances of such soil-nailed structures have been studied in the literature. However, these studies are more concentrated on their characteristics under static loading and only a few studies express their behaviour under dynamic excitations. Different methodologies have been employed to comprehend how soil-nailed structures respond to diverse static and dynamic loadings. It includes field observations, experimental research on reduced scale models and full-scale models, analytical studies and numerical evaluations. Field studies were performed on various nailed structures retaining different soil masses (Felio *et al.* 1990, Hong *et al.* 2005, Li *et al.* 2008, Stocker *et al*. 1979; Wong *et al*. 1997). Felio *et al*. (1990) reported the field behaviour of nailed structures in San Francisco Bay which experienced the 1989 Loma Prieta ground motion. No signs of movement or permanent deformations were observed for soil-nailed structures under dynamic excitation and it was suggested that conservative design as well as construction practice is indispensable for the seismic stability of the structure. The field behaviour of a soil-nailed structure in Singapore constructed for an expressway project to retain a 9m deep excavation cut in residual soil of clayey silt was reported by Wong *et al.* (1997). The maximum lateral wall deformation was found to be less than 0.4% of the wall height after 3 years since the construction and the effectiveness of the method was emphasised under dynamic load cycles without excessive displacements.

Experimental evaluations were carried out using shake table tests and centrifuge tests (Candia *et al.* 2016, El-Emam 2018, Giri and Sengupta 2009, Rotte and Viswanadham 2014, Sahoo *et al.* 2016, Tufenkjian and Vucetic 2000, Wang *et al.* 2010, Yazdandoust 2017, Zhang *et al.* 2014). Giri and Sengupta (2009) through shaking table tests of nailed soil embankment determined that the

*Corresponding author, Research Scholar
E-mail: 23amritar@gmail.com
[a]Professor
[b]Retired Professor

ISSN: 2005-307X (Print), 2092-6219 (Online)

magnitude of non-linear forces developed in nails increased with the increase of slope steepness. The forces were least for nails anchored perpendicular to the slope surface. The crest acceleration was found to decrease with the ascend of slope steepness. The effect of facing was investigated by Rotte and Viswanadham (2014) on the performance of slopes retained by soil nailing through centrifuge tests and numerical studies using finite element software, Plaxis. They reported that the slope facing reduced deformation, improved the stability of the structure and also arrested the local failures of soil between the nails. Zhang *et al*. (2014) concluded that the nailing technique remarkably improved the stability of the structure by restricting the tension cracks of natural slopes, through centrifuge testing on models of reinforced soil-nailed slopes under different loading types which include self-weight, vertical loading and excavation. They determined that nail length further improved the stability resulting in deeper slip surfaces and the nail failure was associated with pull-out failure together with bending deformation. Vucetic *et al.* (1993) performed centrifuge testing on models of soil-nailed excavations and concluded that structures with nail length to wall height ratio higher than 0.67 perform well under cyclic loads.

Juran (1987) discussed the fundamental aspects of the behaviour of nail stabilised structures, soil-nail interaction, soil nailing technology, different structural elements, design methods and construction process involved in soil-nailed retaining structures. It was concluded that the soil-nailed retaining structures were flexible and massive and hence, their resistance to dynamic loads was also high. It was emphasized that the development of the method was empirical and the field experience had significantly preceded the existing theories and fundamental research. Some analytical studies on the performance of nail stabilised slopes under various loads were carried out by Juran *et al*. (1990), Choukeir *et al.* (1997), Jafarbeglou and Kalantary (2023) and Wei *et al*. (2023).

Various computational tools were also utilised by many researchers to comprehend the dynamic characteristics of soil-nailed structures and they concluded that numerical simulations can also offer better insight into the behaviour of nail stabilised retaining structures (Babu and Singh 2008; Briaud and Lim 1997, Dashtara *et al.* 2019, El-Emam 2018, Jianchun and Rong 2012, Kaothon *et al.* 2021, Maleki *et al*. 2023, Manjularani and Manasa 2017, Mohamed *et al*. 2023, Moniuddin *et al*. 2016, Sheikhbahaei *et al.* 2010, Tabaroei *et al.* 2023). Babu and Singh (2008) determined that soil-nailed structures were stable in static and dynamic loading conditions besides attaining the minimal prescribed factor of safety. Dashtara *et al*. (2019) performed a numerical exploration of the deformation and failure mechanism of finite element models of soil-nailed structures under dynamic loads. They reported the optimum inclination of the nail as 20° and suggested a horizontal backslope during excavation to yield minimum displacement. The failure mechanism for a 75° slope was found to be predominantly translational deformations while a 90° slope exhibited a combination of translational and rotational deformations. Singh and Babu (2010) concluded that the behaviour of soil-nailed structures can be properly determined by computational methods only using accurate soil models and mesh density. They highlighted that facing failure can be better understood by considering the bending stiffness of soil nails during analysis.

From an extensive literature review, it is noticed that researches on soil nailing were mostly conducted to examine their effectiveness in stabilising sloped structures. Previous studies have investigated parameters such as nail orientation and nail length under the effect of static loads. Only a handful of studies explored their performance under seismic load conditions in stabilising vertical excavations or cuts made in natural ground. The seismic response analysis of nail stabilised vertical cuts to identify different parameters for stability has not much addressed so far. Hence, this study shifts its focus to evaluating the behaviour of soil-nailed structures by means of numerical simulation and analysis under dynamic loading using the time history of earthquakes and identifying the different parameters for seismic stability. Parametric investigations have been carried out to detect the influence of the orientation of nails with horizontal and the length of nails on the performance of nail stabilised vertical cuts under dynamic load. The effect of the frequency content of dynamic excitation on the behaviour of nailed structures has been also studied. The analysis is further carried through to understand the effectiveness of the soil nailing method on vertical cuts in various site conditions. To accomplish these objectives, vertical 6m high soil-nailed walls in different site classes with various lengths and inclinations of nails subjected to earthquakes are analysed using finite element software, Plaxis 2D (Plaxis 2021).

2. Methodology

To comprehend the characteristics and performance of soil-nailed structures, a soil-nailed wall 6 m high was numerically simulated using Plaxis software and its response under dynamic excitation was analysed for various parameters. The wall was considered vertical with a horizontal backslope. Federal Highway Administration (FHWA) specifications (Lazarte *et al.* 2015) were followed for the design of the 6m high nail stabilised vertical cut. The design was done assuming the length of the nail (L) to be 0.7 times the height of the wall (H) i.e., by taking the L/H ratio as 0.7. The soil nails used in this study were grouted type and the vertical cut was furnished with a facing of 200 mm thickness. The grouted soil nails were placed at a lateral and vertical spacing of 1 m each with the uppermost nail positioned at 0.5 m below the highest point of the vertical cut. Table 1 describes the characteristics of the nail stabilised vertical cut adopted in this study.

Soil nails are usually installed into the soil mass either horizontally or at small inclinations with horizontal. This study was performed to analyse the effect of the inclination of soil nails on the stability of retained soil mass. Nail inclinations (i) of 0, 5, 10, 15 and 20 degrees with horizontal were considered. Based upon the obtained results, the analysis was followed through to identify

Table 1 Characteristics of nail stabilised vertical cut

Description	Value
Vertical cut height (m)	6
Backfill slope (°)	0
Young's modulus of nail, E_n (GPa)	200
Yield strength of nail (MPa)	415
Young's modulus of grout, E_g (GPa)	22
Drilled hole diameter, d_h (mm)	100
Diameter of nail, d (mm)	20
Nail spacing, S_v x S_h (m x m)	1 x 1
Thickness of facing (mm)	200

Table 2 Soil properties (Schanz *et al.* 1999, ASCE7-02 2003, Lazarte *et al.* 2015)

Site Class	C	D	E
Soil description	Very dense soil	Stiff soil	Soft soil
Average shear wave velocity (m/s)	560	270	90
Unit weight (kN/m^3)	20	18	16
Triaxial stiffness modulus (MPa)	1534	334.4	34.35
Oedometer stiffness modulus (MPa)	1227	267.52	27.48
Unloading/ reloading stiffness modulus (MPa)	4602	1003.2	103.05
Angle of friction (°)	40	35	30
Cohesion (kPa)	1	1	1
Dilatancy angle (°)	10	5	0
Poisson's ratio	0.2	0.25	0.3

response variation for various nail lengths and its effect on the stability of the vertical cut. Five nail length to wall height (L/H) ratios of 0.6, 0.7, 0.8, 0.9 and 1 were considered in the study.

A homogeneous soil stratum of soft soil was assumed at the site of excavation. So, the properties of the retained soil and also of the foundation soil were considered the same. Subsequently, analyses were extended for various soil site conditions. The categorisation of soil sites given by the National Earthquake Hazards Reduction Program (NEHRP) (FEMA-450 2003) for seismic design was utilised. The soil sites classified as Class C, Class D and Class E were selected which represent very dense, stiff and soft soil sites, respectively. Table 2 describes the properties of soil considered for numerical simulation.

Boundary analyses were performed and the dimensions of the finite element models were finalised by eliminating the effect of reflection of seismic waves at boundaries on the analysis results. The lateral boundaries were laterally prevented from horizontal movements representing an infinite soil continuum and the bottom boundary was completely fixed. Also, absorbing viscous boundaries were set at the lateral boundaries during dynamic excitations. The schematic representation of geometry for a 6m high nail stabilised vertical cut is demonstrated in Fig. 1. Here, 'H'

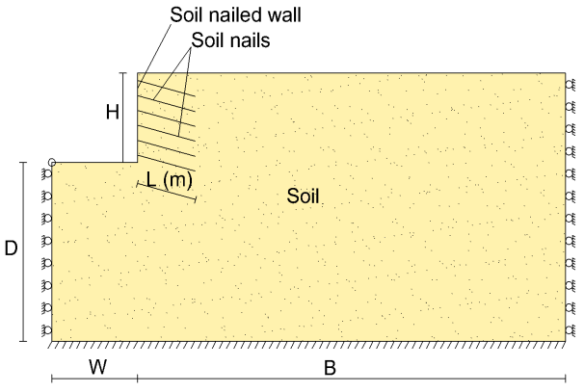

Fig. 1 Schematic representation of nail stabilised vertical cut

Table 3 Natural frequency of soil-nailed structure in various soil sites

Site Class	Natural frequency (Hz)
C	6.2
D	5.2
E	1.3

represents the height of the nailed wall. All other dimensions of the model are denoted with respect to this height of the wall. The excavation width denoted as 'W' was taken as equivalent to the height of the wall (H). The lateral boundaries of the retained soil, denoted as 'B' were ascertained to be spread for a stretch of 5 times the height (5H). The stratum of the foundation soil, D was spread out for a depth of 2 times the wall height (2H).

For the assessment of the seismic stability of nail stabilised vertical cuts under various ground motion excitations, three actual time history earthquake data with scaling were used. To start with dynamic analysis of nail stabilised structure, first, the natural frequency of the nail stabilised vertical cut was determined. The fundamental frequency of soil-nailed models was determined and based on the results, the earthquake data having frequency content corresponding to near-resonant and far-resonant conditions were selected. Free vibration analyses of nailed structures were conducted in various site classes with L/H of 0.7 and nails positioned horizontally. The structure was initially subjected to a prescribed load and a plastic analysis was conducted. This was followed by a dynamic analysis in which the externally applied static load was released and the natural frequency was determined through the power spectral density plot. The natural frequency of the nailed structure in soft soil was obtained as 1.3 Hz. Table 3 lists the results of free vibration analyses carried out in various soil profiles.

The earthquake data used for dynamic analysis were selected based upon the fundamental frequency of the structure. El Centro earthquake (1940) data was taken for analysis which has a high amplitude frequency content of 1.2 Hz, which was close to the natural frequency of the soil-nailed structure in the soft soil profile. The peak ground acceleration (PGA) of the ground motion was scaled down

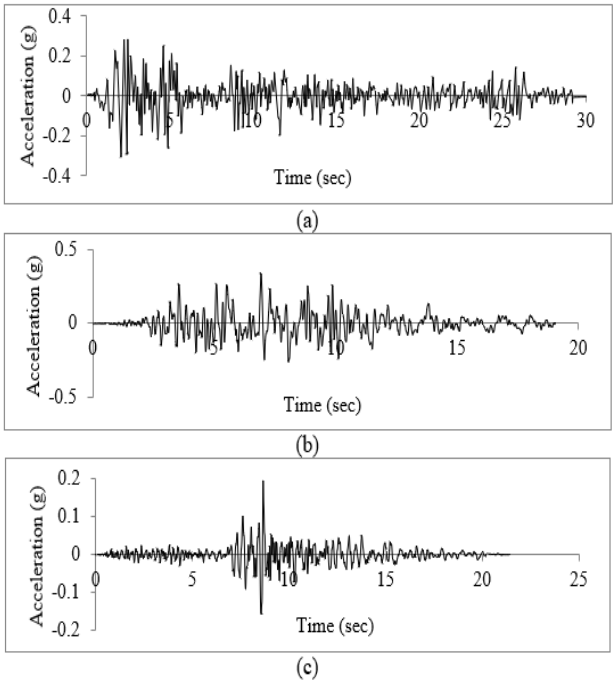

Fig. 2 Actual time history earthquake data pertaining to (a) 1940 El Centro earthquake, (b) 1995 Kobe earthquake and (c) 1983 Trinidad earthquake

to 0.3 g and the total duration of excitation was 20 seconds. The time history data of Kobe earthquake (1995) and Trinidad earthquake (1983) having high amplitude frequency content of 0.59 Hz and 2.8 Hz, respectively representing far resonant earthquakes, were also used in the analysis. All earthquake data were scaled to the same PGA value of 0.3 g to evaluate the influence of the frequency content of excitation solely on the response of the vertical cut. The actual time history of the acceleration of these earthquakes is presented in Fig. 2.

3. Finite element simulation

The numerical simulation of the designed nail stabilised vertical cut was performed employing Plaxis 2D, (Plaxis 2021) which is a finite element software generally utilised to conduct stability, deformation, dynamic and flow analysis for numerous applications in the geotechnical field.

The nail stabilised vertical cut was modelled as a plane strain problem. The modelling of the soil continuum was accomplished using 15-noded triangular elements over 6-noded triangular elements for more accurate results. To properly simulate the behaviour of soil, an appropriate soil model and corresponding material parameters were necessary. Several researchers have used the Hardening soil (HS) model to accurately simulate deep excavations in soil (Bryson and Zapata-Medina 2012, Finno and Calvello 2005, Maleki and Mir Mohammad Hosseini 2022, Pak *et al.* 2021, Zhang *et al.* 2015). As this study deals with the dynamic analyses, the soil mass was modelled as the HS small model. It is an advanced constitutive soil model which uses the theory of plasticity and Mohr-Coulomb failure criteria and is suitable for dynamic simulation of soil. It regards the soil stiffness which is stress dependent and can model both soft and stiff soils. Table 2 lists the properties of soil taken for the analysis and all other input parameters are determined accordingly (Brinkgreve *et al.* 2010, Plaxis 2021, Schanz *et al.* 1999, Yoo *et al.* 2022). The phreatic surface was oriented along the base of the geometry.

Table 4 Numerical input parameters of nail and facing

Parameter	Nail	Facing
Axial stiffness, EA (kN/m)	228.7×10^3	4.4×10^6
Bending stiffness, EI (kNm^2/m)	142.9	14.67×10^3
Poisson's ratio	0.15	0.15

The linear elastic materials were availed for the modelling of the facing and the soil nails. It was simulated employing structural plate elements (Babu and Singh 2008). The main input parameters for the plate element are axial stiffness and flexural rigidity. The soil nail has a circular cross-sectional area comprising of reinforcement bars surrounded by grout thus, the stiffnesses were calculated using the equivalent value of the modulus of elasticity. The equations given below were adopted for the analysis which incorporates the effect of elasticity modulus of both the grout material and the nail (Babu and Singh 2008).

$$\text{Equivalent modulus of elasticity, } E_{eq} = E_n\left(\frac{A_n}{A}\right) + E_g\left(\frac{A_g}{A}\right)$$

$$\text{Axial stiffness, } EA = \frac{E_{eq}}{S_h}\left(\frac{\pi\, {d_h}^2}{4}\right)$$

$$\text{Bending stiffness, } EI = \frac{E_{eq}}{S_h}\left(\frac{\pi\, {d_h}^4}{64}\right)$$

where S_h denotes horizontal spacing of nails, d_h denotes drilled hole diameter, E_g and A_g denote elasticity modulus and cross-sectional area of the grout, E_n and A_n denotes elasticity modulus and cross-sectional area of the nail, and A denotes total cross-sectional area of the grouted nail. Table 4 details the numerical input parameters of soil nail and facing.

Interface elements were provided between plate elements (representing facing and nails) and surrounding soil to enable proper modelling of soil-structure interaction. They consist of virtual thickness that provide a thin layer of intensely shearing materials at the contact region between the plate and the soil. They adopt the material characteristics of the surrounding soil elements, except for the strength reduction factor, R. This factor R was taken as 0.8, which is used in the case of concrete-soil interface (Potyondy 1961). This value determines the strength and stiffness parameters of the interface. After modelling the nail stabilised vertical cut, finite element mesh was generated. Meshing determines the accuracy of numerical analysis results. Finer mesh provides more accurate solutions but, it also consumes more calculation time. For the present study, fine mesh was used for the whole geometry. However, meshing was further refined in the region around the nails and the facing to obtain more accurate results. The initial stresses in the soil layer were

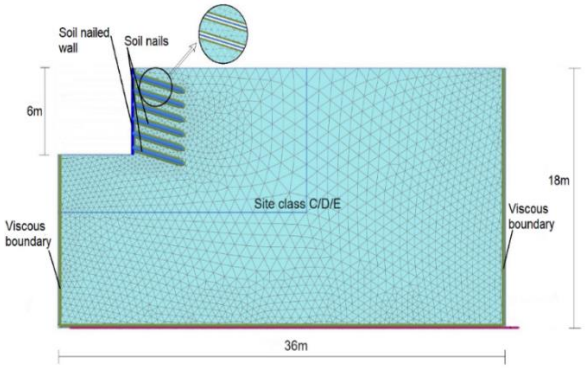

Fig. 3 Finite element mesh of soil-nailed structure

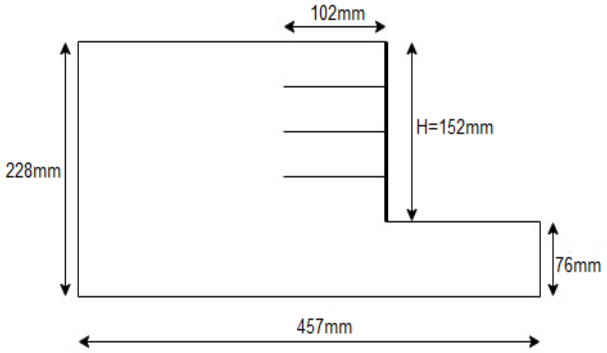

Fig. 4 Longitudinal section of soil-nailed model in dynamic centrifuge test (Vucetic *et al*. 1993)

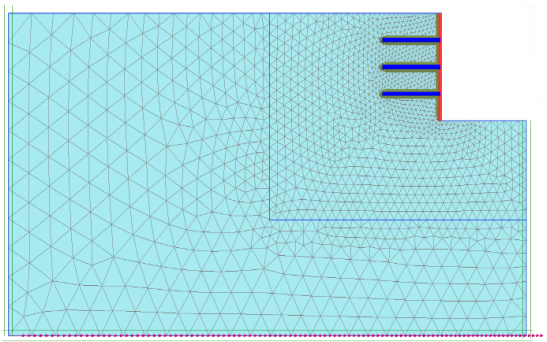

Fig. 5 Meshing of finite element model of soil-nailed model in dynamic centrifuge test

produced using K_o procedure which depicts the at-rest state. Boundary conditions were applied to models simulating the real ground behaviour. The vertical boundaries on the two sides were horizontally restrained from lateral movements and the bottom boundary was fully fixed.

The finite element representation of the 6 m high soil-nailed vertical cut is presented in Fig. 3. The soil nailing method was simulated in stages using an individual phase for each excavation layer. The top to bottom proceeding construction pattern of the technique was simulated in Paxis by deactivating each 1 m layer of soil and activating the nails and facing units contained in that soil layer. This step was continued until the preferred depth of 6 m excavation and construction of the soil-nailed structure was completed.

The dissipation of energy caused due to dynamic loading is generally defined through damping in Plaxis. The material damping is attributed to the viscous properties of the material and the viscous material damping characteristics were simulated through Rayleigh damping. A damping ratio of 5% was assumed and based on the natural frequency of the structure and the frequency of input data, Rayleigh coefficients were calculated. Appropriate boundary conditions guide in avoiding the seismic wave reflection at the end boundaries of the model and the absorption of increment of stresses produced by the dynamic loading which may interrupt the analysis results, thus simulating the actual site behaviour. This was done by providing viscous boundaries for the model at the vertical lateral ends. The viscous boundaries were introduced in Plaxis according to Lysmer and Kuhlmeyer (1969).

The dynamic load was applied at the base of the model in the longitudinal direction through prescribed displacement in the form of the actual time history of earthquake ground motion. El Centro earthquake (1940) data, Kobe earthquake (1995) data and Trinidad earthquake (1983) data were used, scaled to a common PGA of 0.3 g

3.1 Validation of numerical simulation

The validation of the finite element modelling and analysis of the nail stabilised structure using Plaxis was performed using experimental results of centrifuge testing conducted by Vucetic *et al*. (1993). Scaled models of soil-nailed excavations were put through discrete levels of horizontal shaking in centrifuge testing. A scale factor of 50 was utilised for testing. The prototype excavation height (Ĥ) was 7.6 m which was provided with horizontal nails and the length of the nail ranged between 0.33Ĥ and Ĥ. The nails were grouted nails whose prototype diameter was 152 mm. Three rows of nails were provided in a diamond shaped arrangement with nails spaced at 2.5 m and 1.9 m in lateral and vertical direction, respectively. The prototype facing thickness was 160 mm. The cohesion, frictional angle and unit weight of soil used for testing were 7.2 kPa, 36° and 14 kN/m^3, respectively. Fig. 4 shows the representative sketch of the model prepared for the centrifuge test.

Simulation and analysis of the nailed excavation model subjected to dynamic centrifuge tests were performed using Plaxis software. The finite element model of the soil-nailed excavation in centrifuge test is shown in Fig. 5. The length ratio of the nail taken for simulation was 0.76 i.e., L̂/Ĥ = 0.76, where L̂ represents the length of the nail and Ĥ represents the height of the wall. The soil was modelled as an HS small model and the plate elements were employed for modelling facing and nails. The interaction between soil and structural elements was simulated using interface elements. A sinusoidal acceleration of 0.28 g amplitude was applied as the dynamic load.

A comparison among the finite element analysis solutions and those of the experimental findings was made and is presented in Fig. 6. It was noticed that the findings of the numerical analysis were in good conformity with the experimental outcomes and the maximum variation was less than 20%. Hence, similar modelling and analysis employing

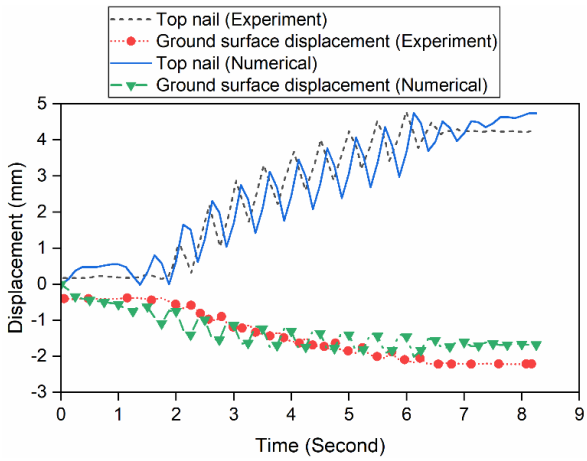

Fig. 6 Comparison of displacement of soil-nailed wall from centrifuge test and finite element analysis

Plaxis software were used in the present work of determining the seismic response evaluation of nail stabilised vertical cuts

4. Results and discussion

To perform dynamic analyses of soil-nailed structures, initially, the free vibration analysis was performed to obtain the fundamental frequency of the nailed structure which is recorded as 1.3 Hz. El Centro ground motion data having a high amplitude frequency content of 1.2 Hz was used for analysis as its frequency content was close to the fundamental frequency of the soil-nailed structure. Different parametric studies were carried out under seismic loading and the results of analyses are discussed below. Results are presented with regard to maximum lateral deformation occurring in the wall, the maximum tensile force developed in the nail, maximum acceleration response of the wall, and lateral earth pressure on the wall under the influence of various nail lengths, nail inclinations and various soil site conditions under three ground motions. For better understanding, the various fixed and variable parameters that were analysed in multiple cases of the numerical analyses are described in Table 5.

4.1 Displacement of soil-nailed wall

Initially, the 6m high vertical cut was simulated and analysed without the stabilisation of the retained mass using soil nails in site Class E under El Centro excitation. The cut was not able to withstand by itself and the failure of soil mass occurred. Thus, it was stabilised using soil nailing and its performance was studied. For evaluating the effect of the inclination of nails, the soil-nailed structures were analysed in Class E soil site with L/H of 0.7 for various nail inclinations 'i' using the time history of El Centro ground motion. Figs. 7(a) and 7(b) show the maximum horizontal deformation recorded in the nailed wall under seismic excitations with various nail inclinations and various nail length ratios, respectively. Horizontal displacement of the wall, denoted as δ is expressed in percentage of the height of the nailed wall (H). The maximum δ is obtained at the wall crest and δ reduces towards the base of the wall.

Fig. 7(a) reveals that the maximum deformation of the vertical cut is recorded for 0º nail inclination (i). It is recorded as 28.35mm at the wall crest which reduces to 22.73mm at the toe of the wall. With the subsequent increase of i from 0° to 15°, the maximum δ of the wall decreases and a further increase of i to 20° results in an increase of δ of the wall. Maximum δ of the nailed wall with 5°, 10°, 15° and 20° nail inclination is 28.08 mm, 27.74 mm, 27.2 mm and 28.2 mm, respectively. The lowest deformation is observed for 15° nail inclination, which is 0.45% of the wall height. Thus, the optimum nail inclination can be concluded as 15° at which δ of the structure is the least under seismic loading. Also, the installation process of nails into the soil mass should be such that it becomes easier to perform. Grouting of nails can be effortless and effective when they are inclined at some angle to the horizontal rather than injecting horizontally. Hence, a nail inclination of 15° can be adopted as it makes the installation process easy and also results in the least horizontal displacement of the structure under dynamic loading. This parametric study has been carried forward with this optimum nail inclination angle of 15°.

The effect of the length of nails on the stability of nail stabilised vertical cuts was studied considering L/H of 0.6, 0.7, 0.8, 0.9 and 1 under dynamic loads with 15° nail inclination. The structure with L/H of 0.5 was also analysed but the length of the nail was not sufficient enough in providing stability to the vertical cut and thus, resulted in the failure of the soil mass. So, L/H starting from 0.6 were employed in this study. Fig. 7(b) displays the maximum δ of the wall for various nail length ratios (L/H), expressed in percentage of the height of the wall (H) for the optimum i of 15°. The results of dynamic analyses show that the lateral movement of the wall is influenced significantly by the nail length.

The deformation is maximum at the wall crest and the magnitude of deformation is highest for L/H of 0.6, which is obtained as 30.7 mm. δ of the wall decreases with the lengthening of the nail. Thus, the least value of δ is obtained for a nail length ratio of 1. Reduction in the magnitude of maximum δ is more when L/H is changed from 0.6 to 0.7 when compared to other subsequent reductions.

This reduction is found to be 11.14% whereas the reduction in maximum δ when L/H is shifted from 0.7 to 0.8 is only 1.75%. The subsequent reductions when L/H is varied from 0.8 to 0.9 and from 0.9 to 1.0 are 2.34% and 5.34%, respectively.

With the lengthening of soil nails, more frictional resistance is obtained at the grout-soil interface making the structure more stable against deformation. The longer nails provide more surface area being in contact with the surrounding soil, which increases the shear resistance along the interface. The lengthening of nails offers a stronger anchorage against the lateral displacement as they penetrate deeper into the soil mass. As a result, the slip surface (potential surface along which soil mass slides or moves) gets deeper into the reinforced soil mass and the structure becomes more resistant against the pull-out failure of nails.

Table 5 Details of combination of parameters

Case	Variable parameters		Fixed parameters			
			Nail inclination (í)	Nail length ratio (L/H)	Site soil class	Input ground motion
1	Nail inclination (í)	0°, 5°, 10°, 15°, 20°	-	0.7	Class E	El Centro
2	Nail length ratio (L/H)	0.6, 0.7, 0.8, 0.9, 1	15°	-	Class E	El Centro
3	Site soil class	C, D, E	15°	0.7	-	El Centro
4	Input ground motion	Kobe, El Centro, Trinidad	15°	0.7	Class E	-

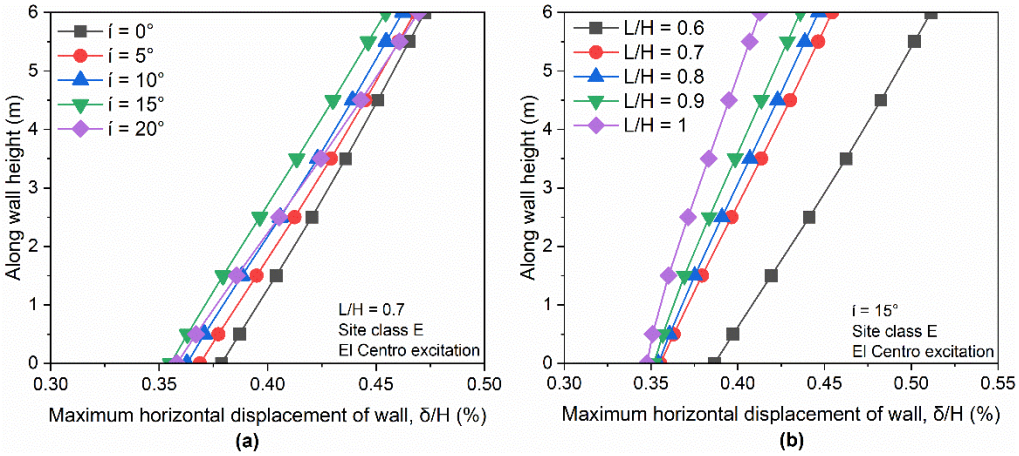

Fig. 7 Maximum lateral deformation in soil-nailed wall for (a) Nail inclinations (í) and (b) Nail length ratios (L/H)

Hence, it is deduced that for better performance and stability of vertical cuts during earthquakes, the structure should have a nail length ratio of 0.7 at least. Increasing L/H beyond 0.7 will further enhance the performance of the nail stabilised structure. The maximum horizontal deformation profile of the finite element model having 15º nail inclination under El Centro earthquake excitation in the soft soil profile for various L/H ratios is illustrated in Fig. 8. The δ is maximum at the wall crest and the deformation pattern consists of two parts having a curved surface followed by a linear one.

The response of the nail stabilised structure was also analysed in various soil site profiles. Three different soil profiles corresponding to site classes C, D and E having shear wave velocity (V_s) 560 m/s (very dense soil), 270 m/s (stiff soil) and 90 m/s (soft soil) were considered in the analyses. Fig. 9(a) shows the maximum δ of the vertical cut along the height of the wall for various soil types. The analyses were carried out with í of 15° and L/H of 0.7. El Centro earthquake data was utilised for dynamic excitation. The graph shows that the displacement is higher in Class E soil site which has lower shear wave velocity in contrast to Class D and Class C with higher shear wave velocities. The deformation of the nailed wall is obtained as 27.2 mm, 21.3 mm and 21.2 mm, respectively in retaining soft, stiff and very dense soil. Since the strength properties of the soft soil are low, the displacement of the vertical cut in such a soil is more critical when subjected to El Centro earthquake excitation. Because of the higher strength properties of soil, the nailed walls in stiff and very dense soil are more stable and thus, exhibit lower deformations. To evaluate the effect of frequency content of dynamic excitation on the stability of the nail stabilised structure, three earthquake data scaled down to a common PGA (0.3 g) (to isolate the effect of acceleration amplitude) were used

As the frequency content of El Centro earthquake data (1.2Hz) is close to the natural frequency of the retained vertical cut (1.3Hz) in the Class E soil profile, the seismic response of the nailed wall is very high for this excitation when compared to the other two earthquake loadings. The frequency content of the Kobe earthquake (0.59Hz) is lower than the fundamental frequency of the nail stabilised cut whereas the Trinidad earthquake has a high amplitude frequency content of 2.8Hz. The analyses were carried out for structures founded in the soft soil profile (Class E) with L/H of 0.7 and í of 15°. The maximum δ of the nailed wall when subjected to three various dynamic excitations is depicted in Fig. 9(b).

It can be observed that δ of the vertical cut is affected based on the frequency content of seismic excitation. The deformation of the wall is less when the frequency content of excitation is high and the deformation is more when the frequency content of excitation is low. The displacement of the wall is maximum when the frequency content of seismic loading is close to the fundamental frequency of the structure. Thus, it can be deduced that under Trinidad excitation having higher frequency content of excitation, the displacement of the wall is less whereas under El Centro excitation which has frequency content close to the fundamental frequency of the structure, the displacement

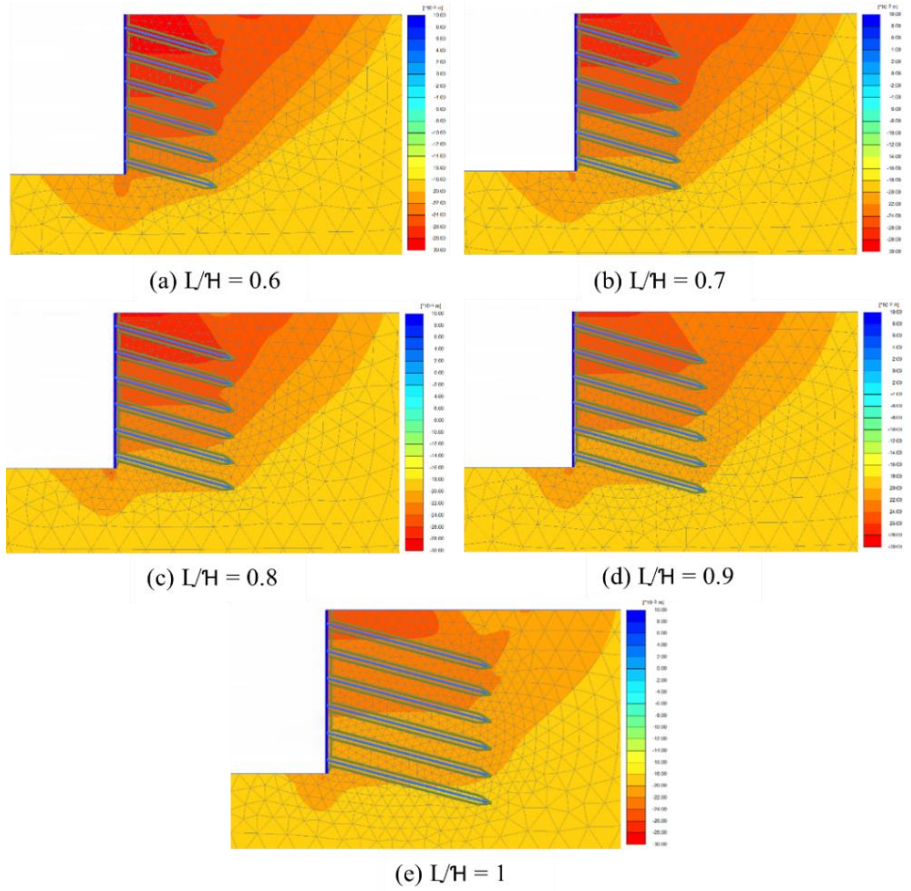

Fig. 8 Maximum horizontal deformation profile of soil-nailed wall in site Class E under El Centro excitation for various L/H ratios

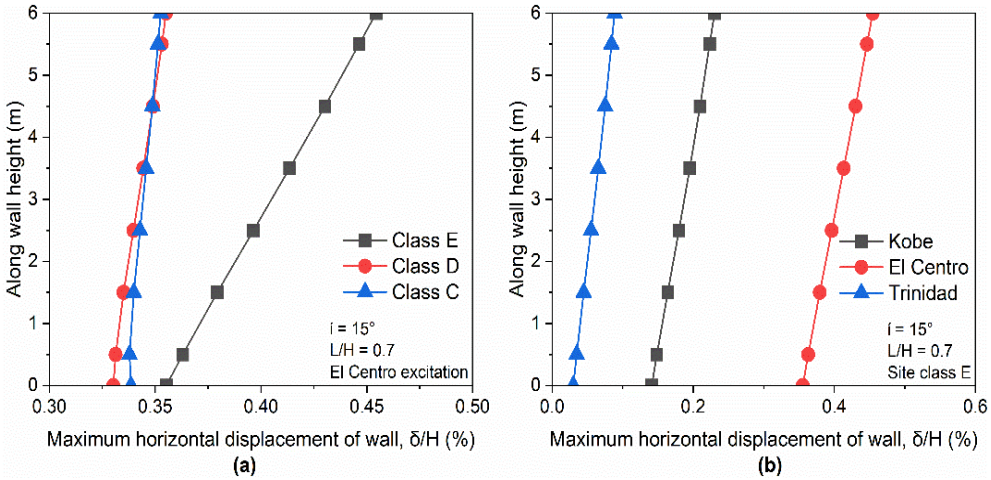

Fig. 9 Maximum lateral deformation in soil-nailed wall for (a) Site classes and (b) Seismic excitations

becomes critical. Kobe excitation results in a lower displacement value of the structure in comparison to El Centro excitation. The time history of δ at the crest of the nail stabilised wall expressed with respect to time, for various nail inclinations, various nail length ratios, various soil site conditions and various earthquake loadings are illustrated in Figs. 10(a)-10(d), respectively. The above discussed results can also be interpreted from these plots.

4.2 Acceleration of soil-nailed wall

The acceleration response of a structure is an important criterion for understanding its behaviour under dynamic loading. The acceleration response exhibited by the wall under dynamic loading for various inclinations of nails (L/H = 0.7) is shown in Fig. 11(a). The acceleration of the wall is observed to have maximum magnitude at the wall

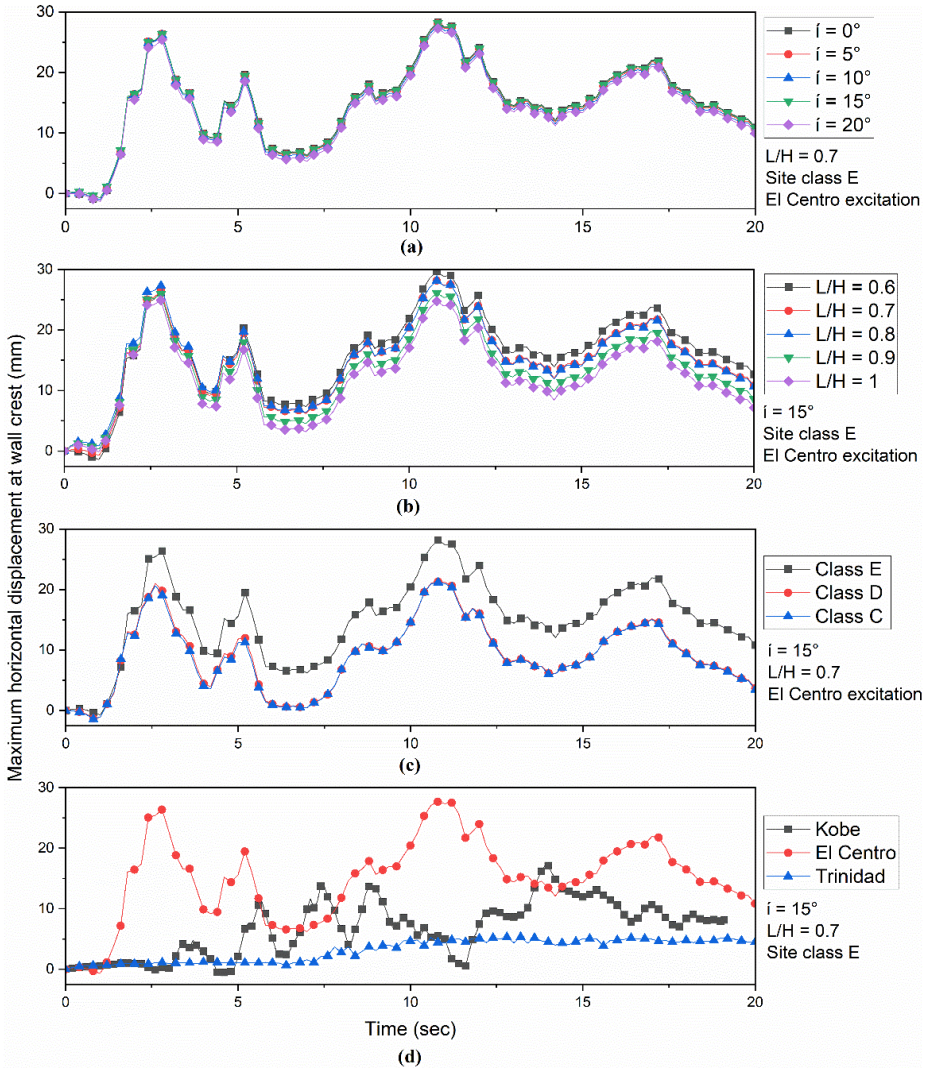

Fig. 10 Time history of horizontal deformation at wall crest for (a) Nail inclinations (í), (b) Nail length ratios (L/H), (c) Site classes and (d) Seismic excitations

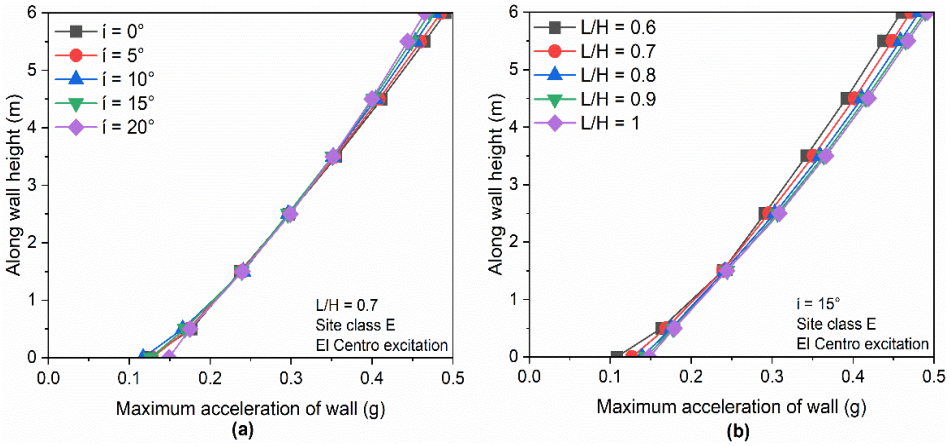

Fig. 11 Maximum acceleration variation in soil-nailed wall for (a) Nail inclinations (í) and (b) Nail length ratios (L/H)

crest which decreases towards the toe, irrespective of the inclination angle of the nail. The graph reveals that there is not much significant variation in the acceleration of the wall despite the change in nail inclination.

However, a slightly higher acceleration value is found for horizontally placed nails and lower acceleration in walls with nails placed at 20° inclination. Fig. 11(b) shows the acceleration distribution of the nail stabilised wall with

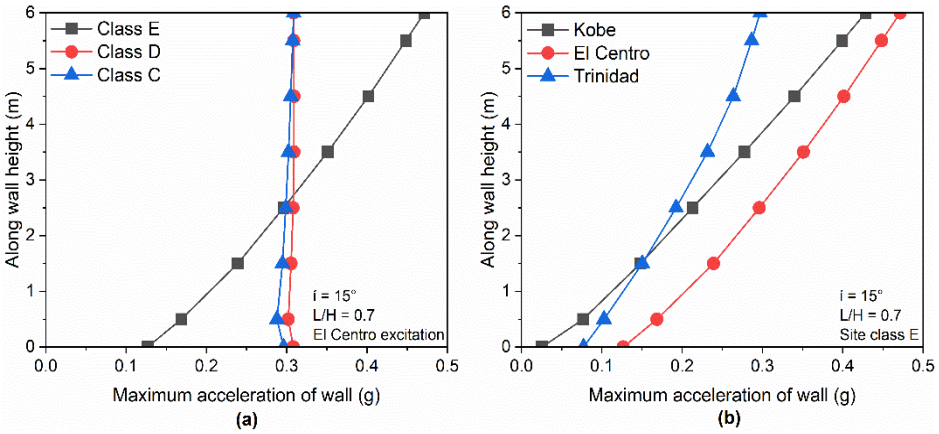

Fig. 12 Maximum acceleration variation in soil-nailed wall for (a) Site classes and (b) Seismic excitations

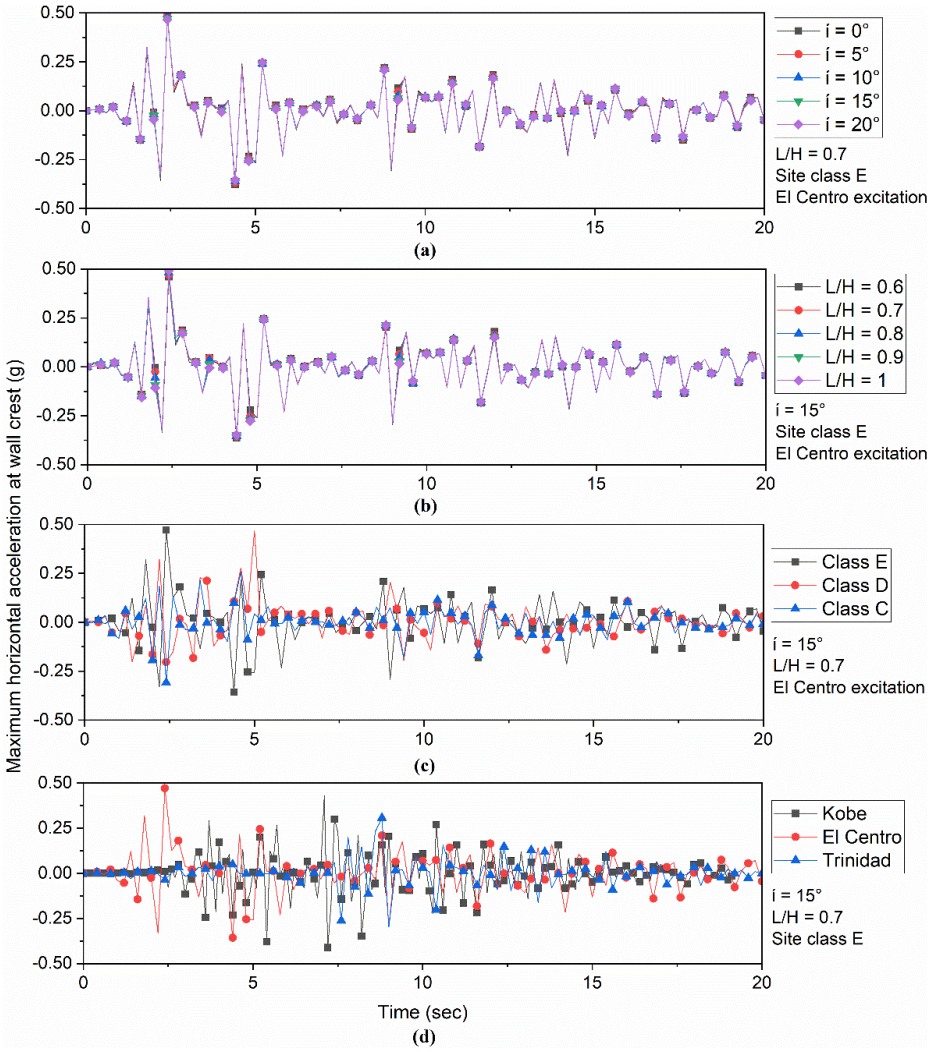

Fig. 13 Acceleration variation at the crest of nailed wall for (a) Nail inclinations (i), (b) Nail length ratios (L/H), (c) Site classes, (d) Seismic excitations

various L/H ratios for i=15°. Even though there are no significant changes in the acceleration of the wall with the lengthening of the nails, it can be noted that the acceleration is minimum when L/H is 0.6. The acceleration increases with the subsequent increase of L/H from 0.6 to 1. Thus, the maximum acceleration of the wall is obtained when the structure consists of the longest nail (L/H = 1).

The acceleration response of structure expressed along the height of the wall for three soil profiles is shown in Fig. 12(a). The soft soil representing Class E soil with low shear

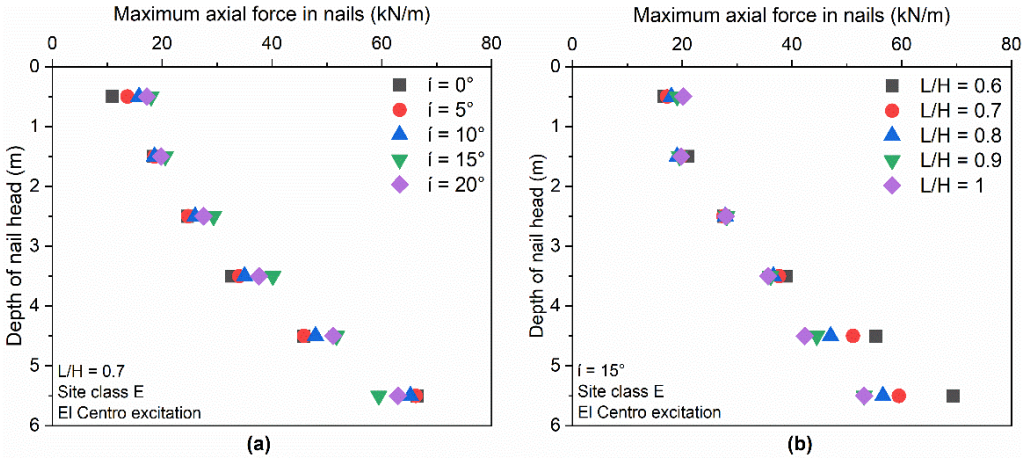

Fig. 14 Maximum axial force variation in nails for (a) Nail inclinations (í) and (b) Nail length ratios (L/H)

wave velocity develops higher acceleration, which decreases from the crest of the wall towards the toe. The stiff soil and very dense soil corresponding to Class D and Class C soil sites display almost similar acceleration responses with nearly a constant value throughout the height of the wall almost close to the applied ground motion. The acceleration of the structure founded in soft soil is more under dynamic excitation compared with other soil sites because of the lower stability of the retained soft soil mass. Class D and Class C site soil have lower deformability characteristics due to higher stiffness thus, they can resist deformation to a greater extent. The stiffness results in maintaining a uniform acceleration profile along the height of the nailed wall. These soils also efficiently propagate shear waves resulting in a uniform distribution of seismic energy within the soil mass and leading to more consistent accelerations along the depth of the nailed wall. Fig. 12(b) shows the acceleration distribution of the nail stabilised vertical cut in the soft soil profile represented as a function of the height of the wall for various seismic excitations. The plot shows that dynamic loading has a profound impact on the acceleration response of the structure. The maximum acceleration is obtained under El Centro earthquake loading when compared to the other two dynamic loadings. Under dynamic excitations with higher and lower frequency content than that of the fundamental frequency of the nail stabilised structure, the acceleration of the wall is found to be less. With the frequency content approaching the fundamental natural frequency of the nail stabilised vertical cut, the wall develops maximum acceleration under the El Centro earthquake. Fig. 13 shows the time history of acceleration response at the crest of the nailed wall for various parameters. It is shown for a duration of 20 seconds

4.3 Axial force in nails

Tensile axial force develops in nails as a consequence of the deformation produced in the soil during dynamic excitation. The maximum tensile force mobilised in different nails under seismic loading for various nail inclinations is expressed along the depth of the nail head as plotted in Fig. 14(a). The magnitude of mobilised maximum tensile nail force increases towards the toe of the nailed wall.

The nails positioned towards the base of the vertical cut developed maximum axial force for every structure as the weight of soil mass increases with the depth. The magnitude of force mobilised for the horizontally placed bottom nail is the highest as more force is generated for the stability of the structure in comparison to other inclinations of nails. The deformation is maximum in this case as a result of which more tensile force is developed in the nails placed horizontally. The deformation of the structure with 15º nail orientation with horizontal was the least, thus the maximum mobilised force in nails under the dynamic load was the minimal for this structure.

Fig. 14(b) shows the variation in the tensile force developed in nails under dynamic excitation for various nail length ratios. Similar to the previous result, the magnitude of axial force mobilised in nails increases with the depth of their installation. Bottom nails are found to develop maximum force in comparison with the nails installed in the upper portion of the vertical cut. This pattern is displayed by all soil-nailed structures irrespective of the length of the nail. However, the maximum magnitude of tensile force is developed in the structure with L/H of 0.6, as it has the lowest nail length and also the structure deforms more under dynamic loading. Thus, it requires more force for stabilising the structure under seismic excitation as a result of which more axial force is mobilised in the corresponding nails. The reduction in the nail force for the bottom nail is 9.18% when L/H is varied from 0.6 to 0.7

With the lengthening of the nail, the tensile nail force increases in the upper half of the vertical cut, while it decreases in the lower half. This trend is consistent with the findings obtained by Yazdandoust (2017).

The locus of maximum nail force at every level of the nail in the vertical cut is shown in Figs. 15(a) and 15(b) for various í and L/H ratios, respectively in site Class E under El Centro ground motion. For soil-nailed structures with nail inclination of 0°, 5° and 10°, the location of maximum tensile force is close to facing for the middle rows of nails. For the top and bottom rows of nails, this position is situated away from the facing. But, for structures with 15°

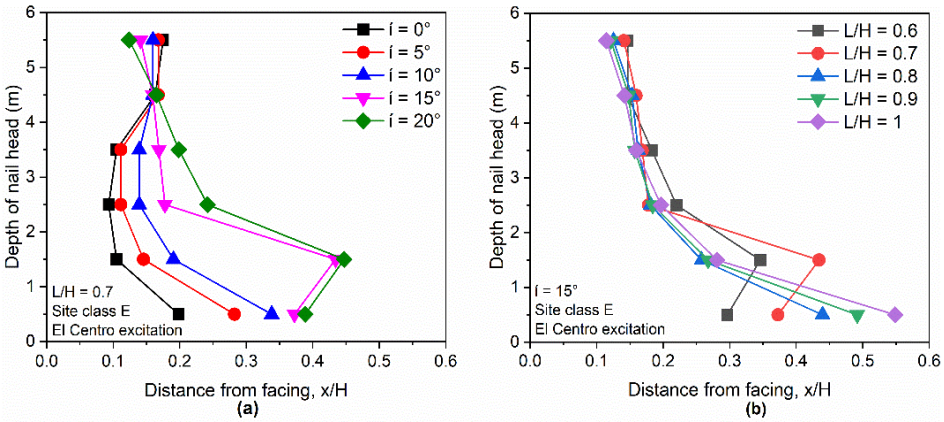

Fig. 15 Location of maximum axial variation in nails for (a) Nail inclinations (i) and (b) Nail length ratios (L/H)

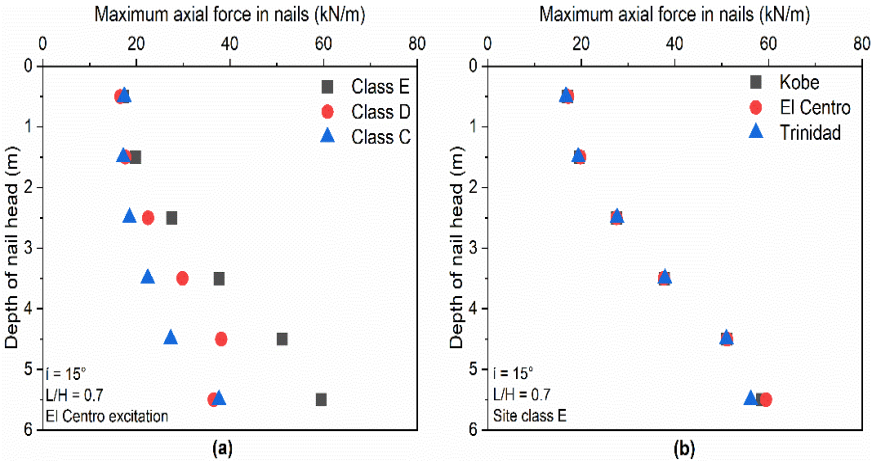

Fig. 16 Maximum axial force variation in nails for (a) Site classes and (b) Seismic excitations

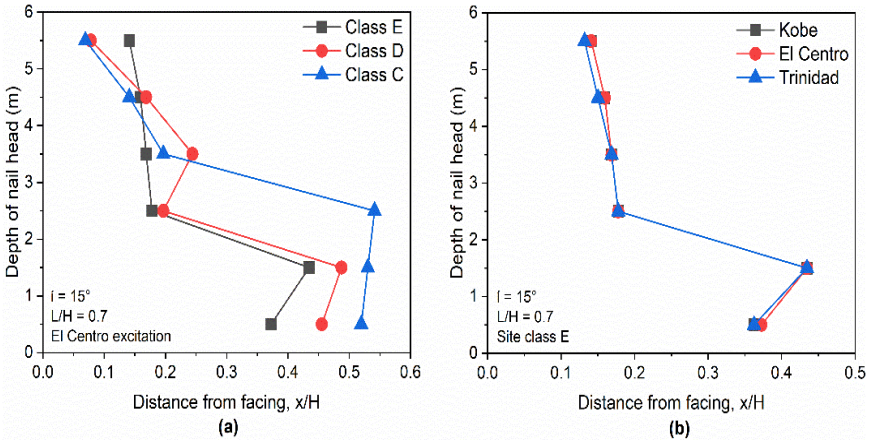

Fig. 17 Location of maximum axial force variation in nails for (a) Site classes and (b) Seismic excitations

and 20° nail inclination, the bottom nails developed maximum axial nail force near the facing. When comparing structures with various L/H, it can be distinguished that for the top row of soil nails, the locus of maximum mobilised axial force is at the far end of the nail from facing. Whereas for bottom rows, it is mobilised at near end of the nail from facing. Thus, from the above results, it is inferred that the nails provided towards the lower portion of the vertical cut play a vital part during seismic excitation and contribute more towards the stability of the structure in comparison to the upper nails.

The axial forces mobilised in nails for the structure retaining various soil profiles under El Centro excitation are shown in Fig. 16(a). The force increases for nails towards the base of the wall and this holds true for all structures irrespective of the soil site condition. A higher magnitude of

Table 6 Various nail forces and their location from the facing

Nail No.	Nail head force (T_o)	Axial force		Shear force		Bending moment	
	(kN/m)	Maximum (kN/m)	Location (m)	Maximum (kN/m)	Location (m)	Maximum (kNm/m)	Location (m)
1	13.51	17.98	2.24	3.67	0	0.99	0
2	14.97	20.58	2.61	11.64	0	2.34	0
3	24.10	29.36	1.07	17.76	0	3.14	0
4	34.16	40.17	1.01	22.95	0	3.68	0
5	45.11	51.78	0.95	25.14	0	3.76	0
6	53.13	59.48	0.90	18.29	0	2.71	0

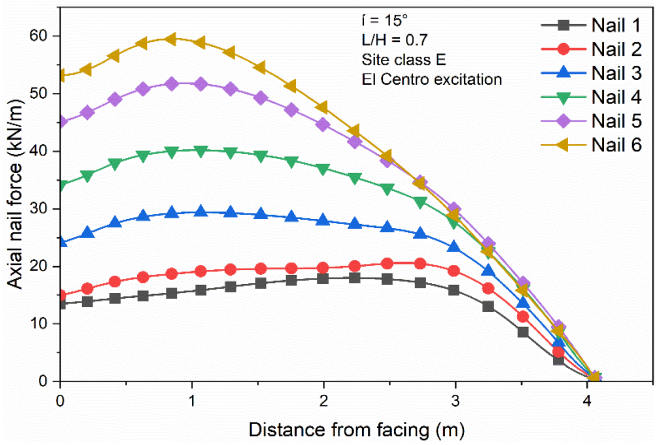

Fig. 18 Tensile axial force along nail lengths for L/H = 0.7 and í = 15° under El Centro excitation in site Class E

nail force is recorded for the bottom nail of the stabilised cut in the case of soft soil corresponding to Class E soil site.

This is attributed to more force requirement of the soft soil for stabilisation under seismic load. With the ascending shear wave velocity of soil, the tensile force mobilised in nails reduces resulting in the development of lowest magnitude of force in very dense soil. The maximum mobilised force in different nails installed at various depths in soft soil profile under various seismic excitations is illustrated in Fig. 16(b). It shows that the development of tensile force in nails during dynamic excitation is not much influenced by the frequency content of excitation. The mobilised force in nails is almost the same under three different earthquake loadings. However, under Trinidad earthquake loading, nails developed a slightly lower magnitude of axial force and El Centro earthquake loading resulted in the development of a slightly higher magnitude of nail force.

Figs. 17(a) and 17(b) show the locus of the maximum tensile force generated in different rows of nails under various soil site profiles and various seismic excitations, respectively. The position of mobilised maximum nail force is found near the facing for nails in the lower portion of the vertical cut in comparison to nails placed in the upper portion of the structure. For every model, this finding is observed to be the same. Thus, it can be perceived that the nails laid towards the lower portion of the wall develop more tensile force and are crucial for the seismic stability of the structure. Fan and Luo (2008) reported that a lower one-third of nails significantly affect the stability of nailed walls, which confirms the findings in this study.

Fig. 18 shows the distribution of tensile force developed along the length of the nails for L/H of 0.7 and í of 15°. The result depicted here is for the structure found in soft soil when subjected to El Centro earthquake loading. All other structures displayed a similar trend for the axial force distribution in nails. Here, the maximum displacement at the wall crest is obtained as 0.45% of the wall height. Nail 1 corresponds to the topmost nail and other nails are numbered sequentially from top to bottom with Nail 6 depicting the bottommost nail. In the uppermost nail (Nail 1), the maximum axial force occurs towards the far end of the nail at a distance of 2.24 m from the facing. With the increase of depth of nail inclusion, this position of maximum force shifts near to the facing side. The bottommost nail (Nail 6) developed maximum force at a distance of 0.9m from the facing. Thus, the topmost nail exhibited maximum axial nail force at a distance of 0.37H from the facing and the bottom most nails developed maximum nail force at 0.15H distance from the facing. These results are consistent with the experimental findings of Byrne *et al.* (1998) who inferred the location of maximum force in top and bottom nails to be at the far end and near end of the nail from facing, respectively.

Table 6 shows the magnitude and position of maximum force variation in the nails for the structure in soft soil

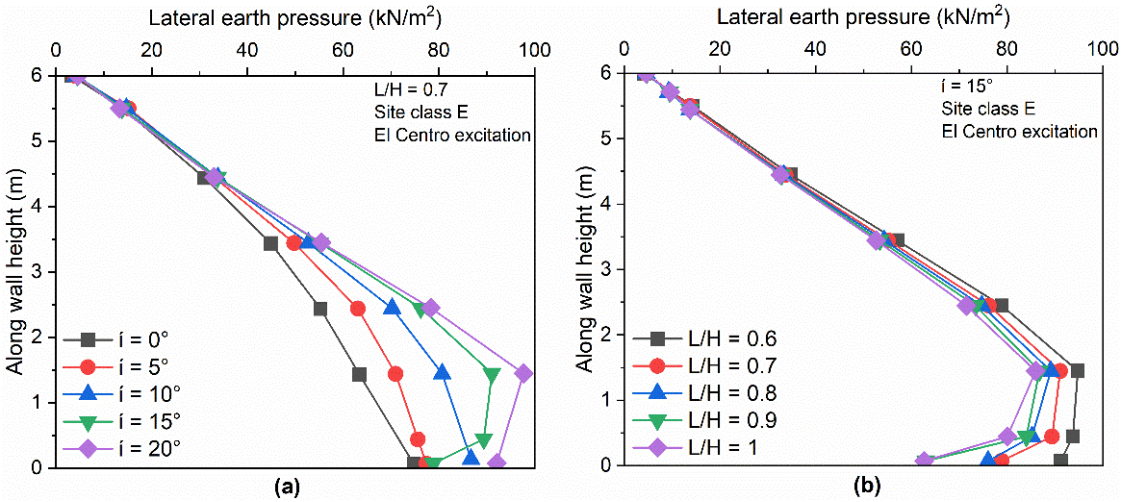

Fig. 19 Lateral earth pressure on soil-nailed wall for (a) Nail inclinations (í) and (b) Nail length ratios (L/H)

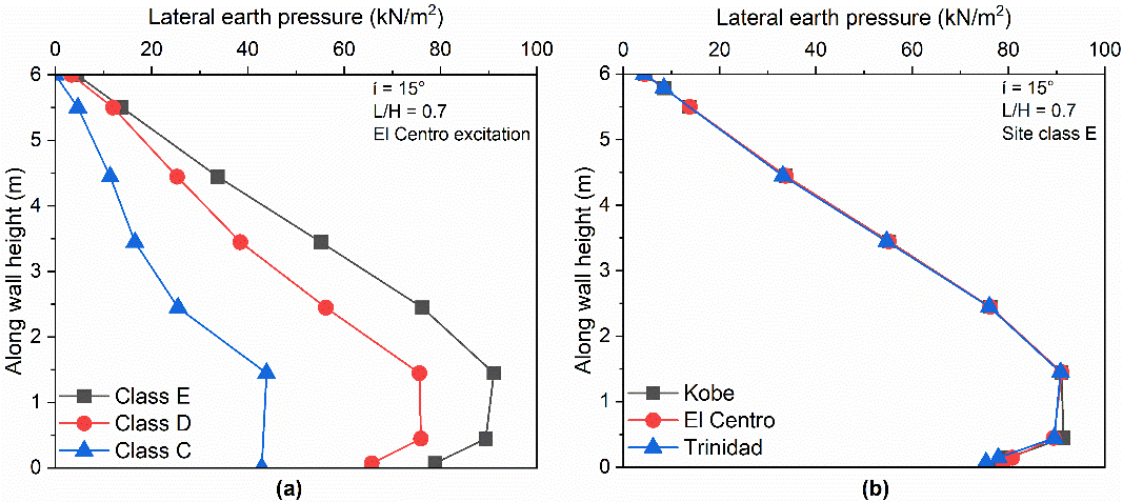

Fig. 20 Lateral earth pressure on soil-nailed wall for (a) Site classes and (b) Seismic excitations

having í of 15° and L/H of 0.7 under El Centro earthquake loading. It can be noticed that the nail force developed at the wall face which is the nail head force (T_o), is about 75 to 89% of the maximum axial force generated in nails.

This result is in harmony with the experimental findings of Byrne *et al.* (1998) who recorded the axial nail head force to be within 60 to 100% of the maximum axial nail force. The higher magnitudes of shear forces and bending moments are developed in the nails at the wall face. This suggests that even though the soil nails are rigidly connected to the facing element, the design of the facing should be properly carried out. Improper design of the facing may result in shear and/or bending failures of the nail at or near the facing.

4.4 Lateral earth pressure dstribution under dynamic loading

The distribution of earth pressure on the soil-nailed wall exerted by the retained soil mass under seismic excitations is described here. Fig. 19(a) displays the lateral earth pressure of soft soil along the wall height under El Centro excitation for various nail inclinations. This earth pressure corresponds to the point of time of the seismic excitation at which the deformation of the nailed wall is maximum. It was observed near 10.8 s of the input ground motion. The pressure distribution shows an increasing trend towards the toe of the wall which is due to an increase in the total weight of soil mass towards the toe of the vertical cut. The distribution of earth pressure of the soil mass on the wall under dynamic loading is non-linear. The pressure is the lowest when the nails are placed in the horizontal direction.

With the increase of orientation of nails with horizontal, the pressure on the nailed wall increases. Thus, maximum lateral earth pressure is provided by the structure with 20° inclined nails. The inclined orientation of nails results in higher confinement of the soil mass, which leads to higher lateral pressure on the wall under the seismic load. The soil pressure rises towards the toe of the vertical cut for í of 0°, 5° and 10°. However, for the inclination of 15° and 20°, the magnitude of pressure first rises and then falls towards the base of the wall. The location of maximum earth pressure is

at a distance of 0.24Ή from the base of the nailed wall for 15° and 20° nail inclinations.

Under El Centro earthquake loading, the earth pressure along the wall height for various L/Ή is shown in Fig. 19(b). The non-linear distribution of dynamic earth pressure exerted by soft soil is shown in the graph. The lateral pressure first increases towards the base and then reduces at the toe of the wall. The maximum pressure is observed at 0.24Ή distance from the base of the stabilised cut, irrespective of the length of the nail. The maximum magnitude of pressure on the wall is recorded for the vertical cut stabilised with L/Ή of 0.6 because it has lower stability in comparison to the structure with other nail length ratios. As a result, during the excitation of the structure under dynamic load, significant movement of soil mass occurs and more force is exerted on the wall by the soil mass. Hence, the pressure is higher for structures with L/Ή of 0.6. The pressure on the wall decreases with the lengthening of the nail and minimum pressure is exerted by the structure with the longest nail. As discussed previously, increasing the length of the nails ensures better penetration into the soil and helps in achieving better anchorage. This enhances the stability of the structure under seismic load and reduces the seismic lateral earth pressure on the wall with longer nails.

A significant change in the magnitude of pressure exerted by the retained soil mass on the nailed wall can be observed in various soil profiles with ί of 15° and L/Ή of 0.7 as shown in Fig. 20(a). The seismic excitation results in dynamic pressure on the wall which is higher in the case of soft soil ground conditions. However, the trend is similar for all three soil profiles. The earth pressure first increases and then decreases towards the toe of the wall. As stiff soil and very dense soil sites are more stable because of high strength properties, the pressure exerted by such soil masses is also less under seismic excitation. Under seismic excitation, the deformation of these soil is less leading to lower lateral seismic pressure on the nailed wall. Fig. 20(b) represents the lateral pressure on the wall when subjected to various seismic excitations for the structure with 15° inclined nails and a length of nail equivalent to 0.7 times the height of the wall. It can be viewed that the pressure distribution of soft soil mass on the wall is not significantly influenced by the change in the frequency content of dynamic excitation. The magnitude and the trend of the lateral earth pressure distribution on the soil-nailed wall are almost the same under Kobe, El Centro and Trinidad earthquake loadings. Similar to previously obtained results, the location of maximum earth pressure is determined to be at 0.24Ή distance from the base of the nailed wall. Even though the frequency content of excitation is different for these three earthquake ground motions, they have the same PGA of 0.3 g. This may be the reason for negligible variation in the lateral pressure distribution on the wall under different seismic loadings. The amplitude of the seismic excitation may influence the intensity of shaking and the resulting lateral earth pressure on the soil-nailed wall rather than the frequency content of excitation.

The present study focuses on evaluating the seismic response of soil-nailed vertical cuts of height 6m comprising of soil nails throughout the structure at a constant nail spacing subjected to scaled real earthquake time history data through an extensive finite element analysis considering many parameters. Hence the results are limited to homogeneous site conditions of medium-rise vertical cuts.

5. Conclusions

The seismic response of a 6m high vertical soil-nailed structure was analysed through numerical computations using Plaxis 2D when subjected to various dynamic excitations and the performance was evaluated for various parameters of nail, soil site profiles and frequency content of dynamic excitations. The conclusions are given below:

- The dynamic stability of the soil-nailed structure is the best with an inclination of nails at 15°.
- With the lengthening of soil nails, the structure becomes more stable against deformation and the failure plane gets deeper into the reinforced soil mass. A minimum nail length ratio of 0.7 is the most suitable under seismic loading conditions. But, the acceleration in wall is not significantly influenced by the length and inclination of the nails.
- Horizontal deformation and acceleration of soil-nailed wall are more for Class E soil site profile.
- As the frequency content of excitation approaches the fundamental frequency of the structure, the response becomes critical. Otherwise, this displacement reduces considerably.
- The tensile force in nails is higher for the nails positioned near the base under dynamic loading. The maximum tensile force in the nail is at the far end from facing for upper nails and at the near end for the bottom nails.
- The dynamic earth pressure distribution on the nailed wall is non-linear and the location of maximum earth pressure occur at 0.24Ή from the base of the vertical cut.

This study recommends a nail inclination of 15º with a nail length ratio of 0.7 for nail stabilised vertical cuts in soft soil under dynamic excitations from the results of extensive numerical analyses.

References

Babu, S.G.L. and Singh, V.P. (2008), "Numerical analysis of performance of soil nail walls in seismic conditions", *ISET J. Earthq. Technol.*, **45**(2), 31-40. Retrieved from https://iset.org.in/public/publications/57237.

Briaud, J.L. and Lim, Y. (1997), "Soil-nailed wall under piled bridge abutment : Simulation and guidelines", *J. Geotech. Geoenviron. Eng.*, **123**(11), 1043-1050. https://doi.org/10.1061/(ASCE)1090-0241(1997)123:11(1043).

Brinkgreve, R.B.J., Engin, E. and Engin, H.K. (2010), "Validation of empirical formulas to derive model parameters for sands", *Numer. Method. Geotech. Eng.*, **1**, 137-142. https://doi.org/10.1201/b10551-25.

Bryson, L.S. and Zapata-Medina, D.G. (2012), "Method for estimating system stiffness for excavation support walls", *J.*

Geotech. Geoenviron. Eng., **138**(9), 1104-1115. https://doi.org/10.1061/(asce)gt.1943-5606.0000683.

Byrne, R.J., Cotton, D., Porterfield, J., Wolschlag, C. and Ueblacker, G. (1998), "Manual for design and construction monitoring of soil nail walls", Report No. FHWA-SA-96-69R; Fedeal Highway Administration, Washington, DC.

Candia, G., Mikola, R.G. and Sitar, N. (2016), "Seismic response of retaining walls with cohesive backfill: Centrifuge model studies", *Soil Dyn. Earthq. Eng.*, **90**, 411-419. https://doi.org/10.1016/j.soildyn.2016.09.013.

Choukeir, M., Juran, I. and Hanna, S. (1997), "Seismic design of reinforced-earth and soil-nailed structures", *Ground Improvement*, **1**(4), 223-238. https://doi.org/10.1680/gi.1997.010404.

Dashtara, H., Kolahdouzan, A.H., Saeedi-Azizkandi, A. and Baziar, M.H. (2019), "Numerical investigation on the displacements and failure mechanism of soil-nailed structures in seismic conditions", *Proceedings of the 8th International Conference on Case Histories in Geotechnical Engineering, Geo-Congress*, Philadelphia, Pennsylvania.

El-Emam, M.M. (2018), "Experimental verification of current seismic analysis methods of reinforced soil walls", *Soil Dyn. Earthq. Eng.*, **113**, 241-255. https://doi.org/10.1016/j.soildyn.2018.06.006.

Fan, C.C. and Luo, J.H. (2008), "Numerical study on the optimum layout of soil-nailed slopes", *Comput. Geotech.*, **35**(4), 585-599. https://doi.org/10.1016/j.compgeo.2007.09.002.

Felio, G.Y., Vucetic, M., Hudson, M., Barar, O. and Chapman, R. (1990), "Performance of soil nailed walls during the October 17, 1989 Loma Prieta Earthquake", *Proceedings of the 43rd Canadian Geotechnical Conference*, Quebec, Canada.

FEMA-450 (2003), "NEHRP recommended provisions for seismic regulations for new buildings and other structures", Building Seismic Safety Council for the Federal Emergency Management Agency; Washington, DC, USA.

Finno, R.J. and Calvello, M. (2005), "Supported excavations: observational method and inverse modeling", *J. Geotech. Geoenviron. Eng.*, **131**(7), 826-836. https://doi.org/10.1061/(asce)1090-0241(2005)131:7(826).

Giri, D. and Sengupta, A. (2009), "Dynamic behavior of small scale nailed soil slopes", *Geotech. Geol. Eng.*, **27**(6), 687-698. https://doi.org/10.1007/s10706-009-9268-x.

Hong, Y.S., Chen, R.H., Wu, C.S. and Chen, J.R. (2005), "Shaking table tests and stability analysis of steep nailed slopes", *Can. Geotech. J.*, **42**(5), 1264-1279. https://doi.org/10.1139/t05-055.

Jafarbeglou, M. and Kalantary, F. (2023), "Probabilistic optimization of nailing system for soil walls in uncertain condition", *Geomech. Eng.*, **34**(6), 597-609. https://doi.org/10.12989/gae.2023.34.6.597.

Jianchun, W. and Rong, S. (2012), "Seismic analysis of soil nailed wall using finite element method", *Adv. Mater. Res.*, **535**, 2027-2031. https://doi.org/10.4028/www.scientific.net/AMR.535-537.2027.

Juran, I. (1987), "Nailed-soil retaining structures : Design and practice", *Transport. Res. Record*, (1119), 139-150.

Juran, I., Baudrand, G., Farrag, K. and Elias, V. (1990), "Kinematical limit analysis for design of soil-nailed structures", *J. Geotech. Eng.*, **116**(1), 54-72. https://doi.org/10.1061/(ASCE)0733-9410(1990)116:1(54).

Kaothon, P., Chhun, K.T. and Yune, C.Y. (2021), "Numerical evaluation on steep soil - nailed slope using finite element method", *Int. J. Geo-Eng.*, **12**, 1-12. https://doi.org/10.1186/s40703-021-00159-y.

Lazarte, C.A., Robinson, H., Gomez, J.E., Baxter, A., Cadden, A. and Berg, R. (2015), "Geotechnical engineering circular No. 7 soil nail walls reference manual", Developed following: AASHTO LRFD Bridge Design Specifications, 7th Ed., No. FHWA-NHI-14-007; National Highway Institute, US Department of Transportation Federal Highway Administration, Washington, DC.

Li, J., Tham, L.G., Junaideen, S.M., Yue, Z.Q. and Lee, C.F. (2008), "Loose fill slope stabilization with soil nails: Full-scale test", *J. Geotech. Geoenviron. Eng.*, **134**(3), 277-288. https://doi.org/10.1061/ASCE1090-02412008134:3277.

Lysmer, J. and Kuhlmeyer, R.L. (1969), "Finite element method for infinite media", *J. Eng. Mech.*, **95**, 859-877. https://doi.org/10.1061/JMCEA3.0001144.

Maleki, M. and Mir Mohammad Hosseini, S.M. (2022), "Assessment of the Pseudo-static seismic behavior in the soil nail walls using numerical analysis", *Innov. Infrastruct. Solutions*, **7**(4), 262. https://doi.org/10.1007/s41062-022-00861-5.

Maleki, M., Khezri, A., Nosrati, M., Majdeddin, S. and Mohammad, M. (2023), "Seismic amplification factor and dynamic response of soil - nailed walls", *Model. Earth Syst. Environ.*, **9**(1), 1181-1198. https://doi.org/10.1007/s40808-022-01543-y.

Manjularani, P. and Manasa, C.K. (2017), "Static and dynamic analysis of soil nail wall and retaining wall for vertical cut", *Proceedings of the International Conference on Current Trends in Engineering, Science and Technology*. https://doi.org/10.21647/icctest/2017/49058.

Mohamed, M.H., Ahmed, M. and Mallick, J. (2023), "Finite element modeling of the soil-nailing process in nailed-soil slopes", *Appl. Sci.*, **13**(4), 2139. https://doi.org/10.3390/app13042139.

Moniuddin, M.K., Manjularani, P. and Govindaraju, L. (2016), "Seismic analysis of soil nail performance in deep excavation", *Int. J. Geo-Eng.*, **7**(1), 1-10. https://doi.org/10.1186/s40703-016-0030-y.

Pak, A., Maleki, J., Aghakhani, N. and Yousefi, M. (2021), "Numerical investigation of stability of deep excavations supported by soil-nailing method", *Geomech. Geoeng.*, **16**(6), 434-451. https://doi.org/10.1080/17486025.2019.1680878.

Plaxis (2021), *2D Reference manual*, *Version V21*, PLAXIS BV, Delft, The Netherlands.

Potyondy, J.G. (1961), "Skin friction between various soils and construction materials", *Géotechnique*, **11**(4), 339-353.

Rabcewicz, L.V. (1964), "The new Austrian tunnelling method. part I", *Water Power*, **16**, 453-457.

Rotte, V.M. and Viswanadham, B.V.S. (2014), "Centrifuge and numerical model studies on the behaviour of soil-nailed slopes with and without slope facing", *Tunn. Undergr. Constr.*, **242**, 581-591. https://doi.org/10.1061/9780784413449.056.

Sahoo, S., Manna, B. and Sharma, K.G. (2016), "Seismic stability analysis of un-reinforced and reinforced soil slopes", *Geo-China*, **3**, 74-81. https://doi.org/10.1061/9780784480007.009.

SCE 7-16 (2016), Minimum Design Loads for Buildings and Other Structures, American Society of Civil Engineers/Structural Engineering Institute; Reston, VA.

Schanz, T., Vermeer, P.A. and Bonnier, P.G. (1999), "The hardening soil model : Formulation and verification", *Beyond 2000 in Computational Geotechnics – 10 Years of PLAXIS © 1999 Balkema, Rotterdam, Netherlands*, 1-16. https://doi.org/10.1201/9781315138206-27.

Sheikhbahaei, A., Halabian, A.M. and Hashemolhosseini, S.H. (2010), "Analysis of soil nailed walls under seismic excitations using finite difference method", *Proceedings of the 5th International Conference on Recent Advances in Geotechnical Earthquake Engineering and Soil Dynamics*, San Diego, California.

Singh, V.P. and Babu, S.G.L. (2010), "2D Numerical simulations of soil nail walls", *Geotech. Geol. Eng.*, **28**(4), 299-309.

https://doi.org/10.1007/s10706-009-9292-x.

Stocker, M.F., Korber, G.W., Gassler, G. and Gudehus, G. (1979), "Soil nailing", *Proceedings of the International Conference on Soil Reinforcement*, Paris, France.

Tabaroei, A., Seyedi, S.T. and Pouraminian, M. (2023), "Performance of a Deep Excavation Reinforced by Soil-Nailing During an Earthquake Excitation", *Iranian J. Sci. Technol. Transact. Civil Eng.*, **47**, 3021–3031. https://doi.org/10.1007/s40996-023-01094-x.

Tufenkjian, M.R. and Vucetic, M. (2000), "Dynamic failure mechanism of soil-nailed excavation models in centrifuge", *J. Geotech. Geoenviron. Eng.*, **126**(3), 227–235. https://doi.org/10.1061/(ASCE)1090-0241(2000)126:3(227).

Vucetic, M., Tufenkjian, M.R. and Doroudian, M. (1993), "Dynamic centrifuge testing of soil-nailed excavations", *Geotech. Test. J.*, **16**(2), 172-187. https://doi.org/10.1520/GTJ10034J.

Wang, L., Zhang, G. and Zhang, J.M. (2010), "Nail reinforcement mechanism of cohesive soil slopes under earthquake conditions", *Soils Found.*, **50**(4), 459-469. https://doi.org/10.3208/sandf.50.459.

Wei, X., Zou, J. and Chen, G. (2023), "Seismic stability analysis of heterogeneous slopes reinforced by inclined soil nails", *Eur. J. Environ. Civil Eng.*, **27**(16), 4544-4562. https://doi.org/10.1080/19648189.2023.2194938.

Wong, I.H., Low, B.K., Pang, P.Y. and Raju, G.V.R. (1997), "Field performance of nailed soil wall in residual soil", *J. Perform. Constr. Fac.*, **11**(3), 105-112. https://doi.org/10.1061/(ASCE)0887-3828(1997)11:3(105).

Yazdandoust, M. (2017), "Experimental study on seismic response of soil-nailed walls with permanent facing", *Soil Dyn. Earthq. Eng.*, **98**, 101-119. https://doi.org/10.1016/j.soildyn.2017.04.009.

Yoo, M., Kwon, S.Y. and Hong, S. (2022), "Dynamic response evaluation of deep underground structures based on numerical simulation", *Geomech. Eng.*, **29**(3), 269-279. https://doi.org/10.12989/gae.2022.29.3.269.

Zhang, G., Cao, J. and Wang, L. (2014), "Failure behavior and mechanism of slopes reinforced using soil nail wall under various loading conditions", *Soils Found.*, **54**(6), 1175-1187. https://doi.org/10.1016/j.sandf.2014.11.011.

Zhang, W., Goh, A.T.C. and Xuan, F. (2015), "A simple prediction model for wall deflection caused by braced excavation in clays", *Comput. Geotech.*, **63**, 67-72. https://doi.org/10.1016/j.compgeo.2014.09.001.